PAUL SCHERRER INSTITUT

A. Vasiliev, H. Ferroukhi, M. Pecchia, D. Rochman, A. Pautz :: Paul Scherrer Institut
and A. Laureau, V. Lamirand (EPFL)

Revision of PSI calculation capabilities and validation experience on the BEPU-type reactor dosimetry applications

17th International Symposium on Reactor Dosimetry
EPFL, Lausanne, 21-26 May 20233.

Laboratory for
Reactor Physics and Thermal-Hydraulics

Current status of the LRT/PSI FNF calculation methodology

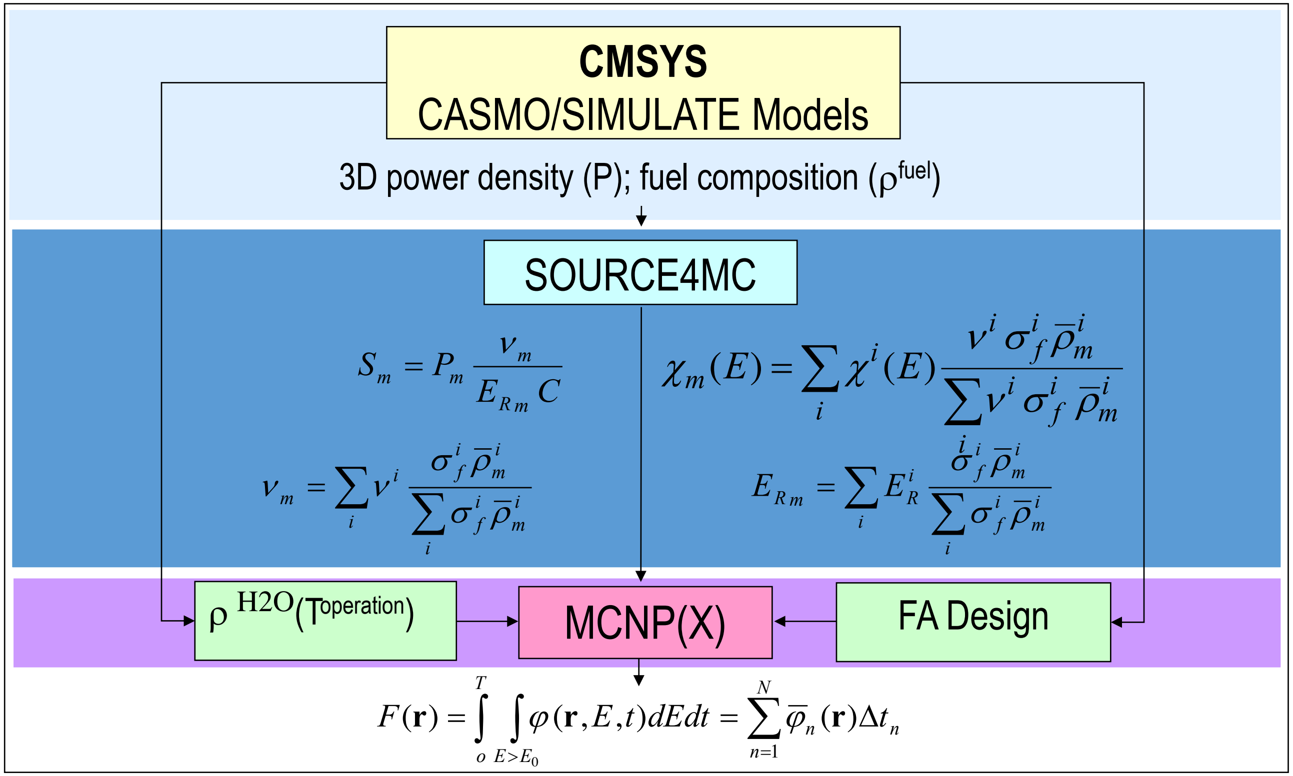

A 2D-1D synthesized approach employed for the neutron source strength specifications at each fuel assembly level: 2D radial pin-wise distributions with laterally-averaged 1D axial distributions. The 2D spectrum specifications were based on the FA-average major fissionable nuclides concentrations.

Extensions towards shielding and activation simulations

Employment of ADVANTG for VR

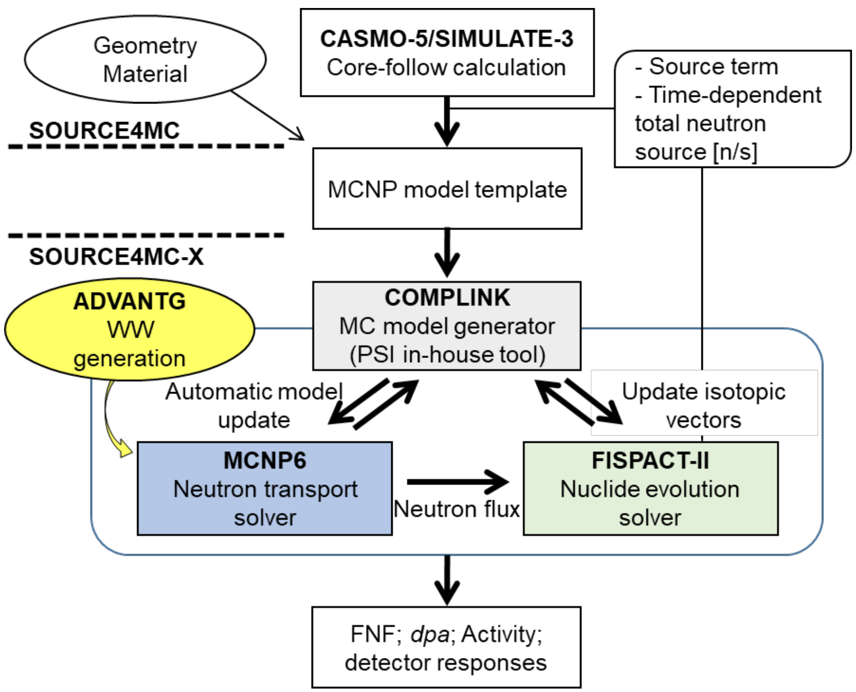

Coupling with FISPACT-II

LRT methodology for ECD WF based on Green's function evaluation using MCNP PTRAC file

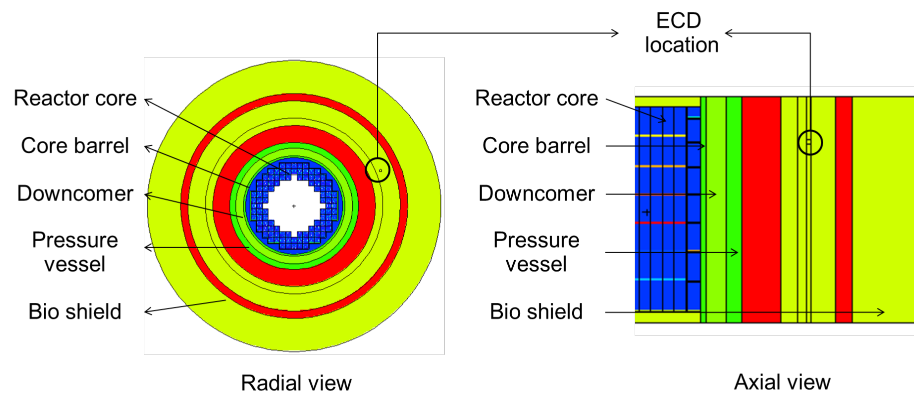

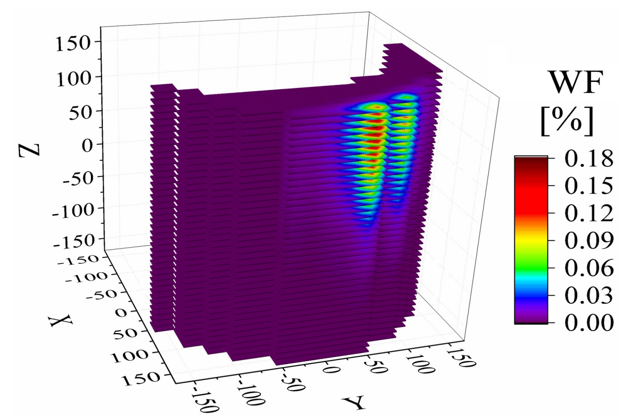

Allows evaluation of 3D importance maps upon a user defined grid using a single MCNP run

PSI NDUQ tool NUSS for MC simulations

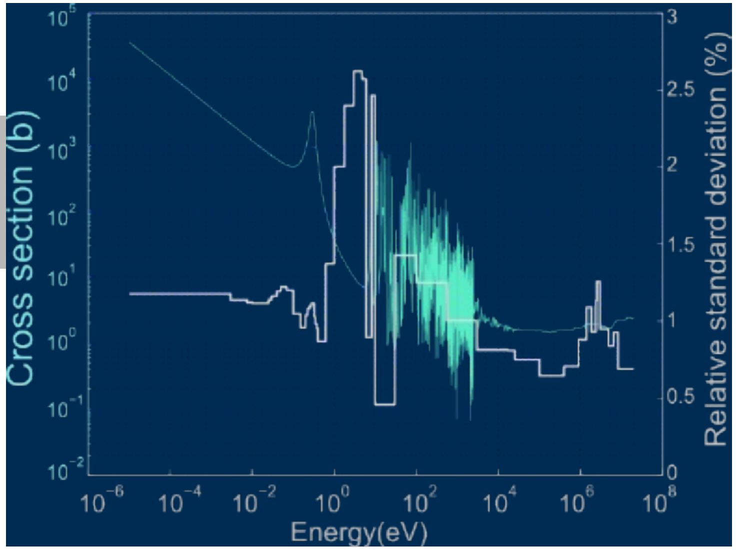

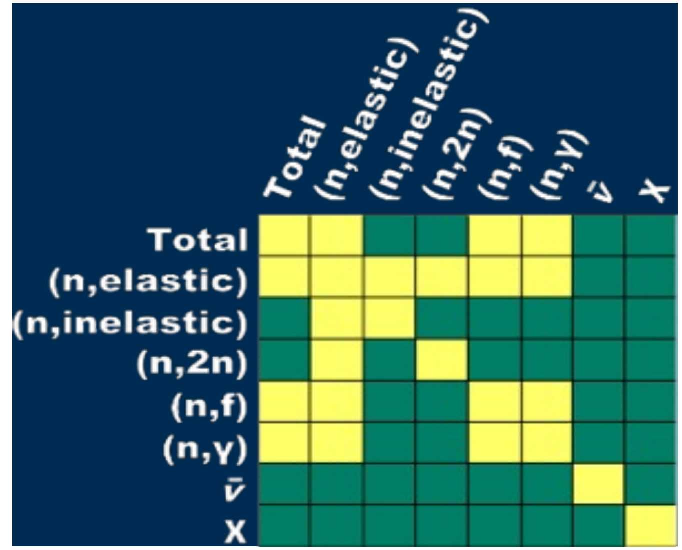

Nuclear data format	Uncertainty format	Global (sampling)	Local (SCST)
Basic data	Basic data	TMC	
Evaluated data	Evaluated data	NUDUNA	
Pointwise	Multigroup	**NUSS** ✓ MCNPX	pert card MCNP6 KSEN McCARD MVP
Multigroup		XSUSA	TSUNAMI-3D MMKKENO

Illustration on the dosimetry experimental data available at PSI

Swiss ‘Pre-convoy’ 3-loops 3000MWt PWR (KKG)

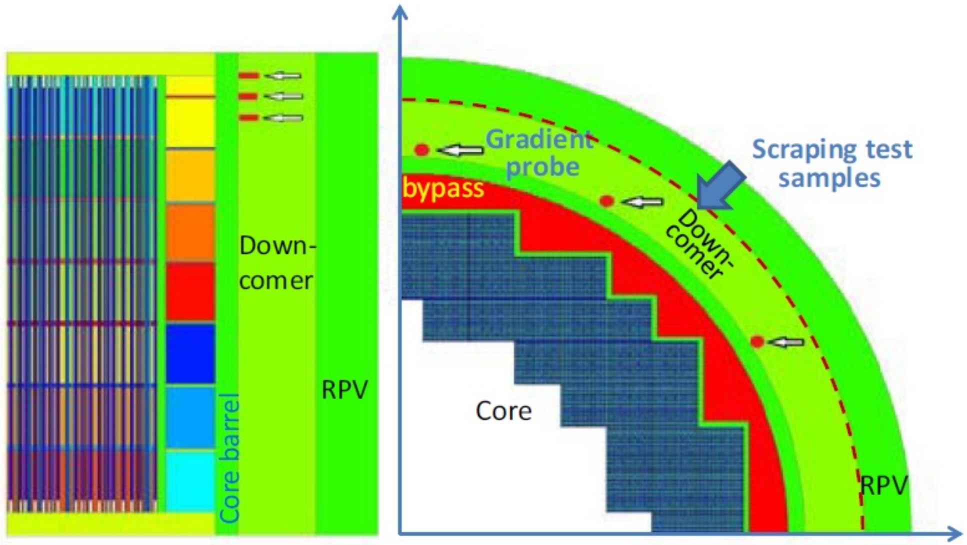

After 27 cycles

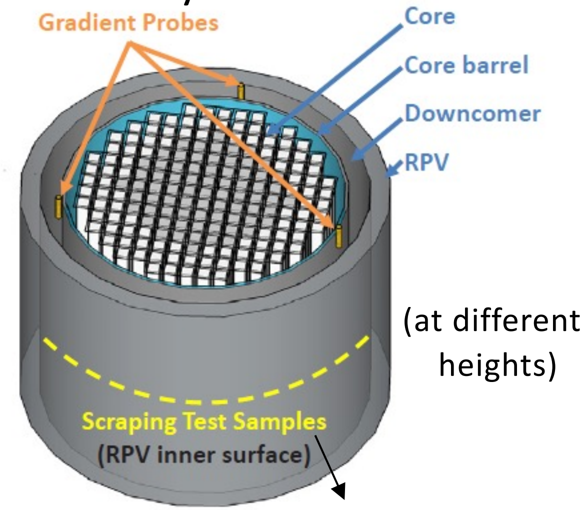

After 10 & 27 cycles

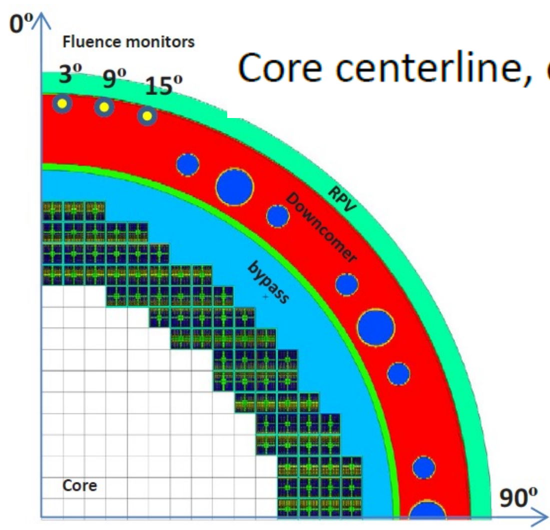

Core centerline, different azimuths

GE 3600MWt BWR/6 (KKL)

Sinbad HBR-II and PCA-Replica benchmark models complementing the PSI validation database

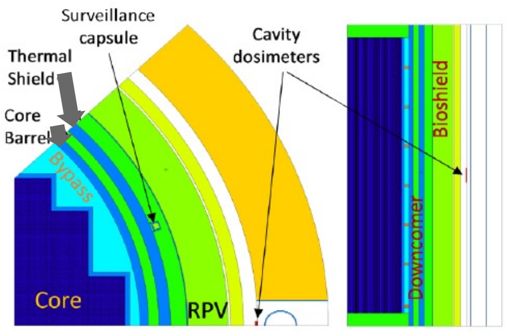

Illustration of the H.B. Robinson-II RPV Dosimetry Benchmark, as modelled with MCNPX.

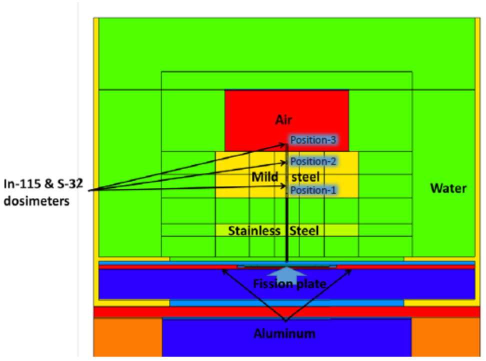

Illustration on of the PCA-Replica MCNP calculation model.

Correlations between PWR FNF and the dosimetry reaction rates for the considered models.

Swiss PWR	HBR2-capsule						HBR2-cavity					
	Np-237	U- 238	Ni-58	Fe-54	Ti-46	Cu-63	Np-237	U-238	Ni-58	Fe-54	Ti-46	Cu-63
PWR_Barrel	0.94	0.89	0.74	0.71	0.51	0.37	0.80	0.72	0.59	0.49	0.27	0.20
	[0.92, 0.95]	[0.86, 0.91]	[0.68, 0.79]	[0.64, 0.76]	[0.42, 0.60]	[0.26, 0.47]	[0.75, 0.84]	[0.66, 0.78]	[0.50, 0.66]	[0.40, 0.58]	[0.15, 0.38]	[0.08, 0.31]
PWR_RPV	0.93	0.91	0.81	0.78	0.63	0.52	0.81	0.78	0.74	0.66	0.45	0.37
	[0.91, 0.94]	[0.89, 0.93]	[0.76, 0.85]	[0.73, 0.82]	[0.55, 0.70]	[0.42, 0.60]	[0.77, 0.85]	[0.73, 0.83]	[0.68, 0.79]	[0.59, 0.72]	[0.35, 0.54]	[0.26, 0.47]
PWR_BIO1	0.88	0.88	0.75	0.71	0.60	0.52	0.87	0.91	0.82	0.73	0.50	0.43
	[0.84, 0.90]	[0.85, 0.90]	[0.69, 0.80]	[0.65, 0.77]	[0.52, 0.68]	[0.42, 0.60]	[0.84, 0.90]	[0.89, 0.93]	[0.78, 0.86]	[0.66, 0.78]	[0.41, 0.59]	[0.32, 0.52]
PWR_BIO2	0.60	0.65	0.76	0.76	0.73	0.66	0.44	0.48	0.82	0.83	0.73	0.66
	[0.51, 0.67]	[0.57, 0.72]	[0.70, 0.80]	[0.70, 0.80]	[0.67, 0.78]	[0.59, 0.72]	[0.34, 0.54]	[0.38, 0.57]	[0.77, 0.85]	[0.79, 0.87]	[0.67, 0.78]	[0.58, 0.72]

Swiss PWR	PCA-REPLICA					
	1_In-115	1_S-32	2_In-115	2_S-32	3_In-115	3_S-32
PWR_Barrel	0.70	0.54	0.67	0.48	0.63	0.42
	[0.63, 0.76]	[0.45, 0.62]	[0.60, 0.73]	[0.38, 0.57]	[0.56, 0.70]	[0.32, 0.52]
PWR_RPV	0.87	0.78	0.82	0.74	0.77	0.68
	[0.84, 0.90]	[0.72, 0.82]	[0.77, 0.85]	[0.68, 0.79]	[0.71, 0.81]	[0.61, 0.74]
PWR_BIO1	0.84	0.70	0.88	0.76	0.87	0.73
	[0.80, 0.87]	[0.63, 0.76]	[0.85, 0.91]	[0.70, 0.81]	[0.84, 0.90]	[0.67, 0.78]
PWR_BIO2	0.58	0.77	0.47	0.85	0.43	0.83
	[0.50, 0.66]	[0.71, 0.81]	[0.37, 0.56]	[0.81, 0.88]	[0.32, 0.52]	[0.79, 0.86]

Summary of the LRT/PSI LWR dosimetry validation database

Experimental data source	Identification	N. of irrad. cycles	Detectors	C/E sample size
Swiss PWR/ PSI NES Hotlab	RPV Scraping test 1 [2]	21	^{93}Nb(n,n')^{93m}Nb	12
	RPV Scraping test 2 [7], 4 out of 27 elevations not included	27	^{54}Fe(n,p)^{54}Mn; ^{93}Nb(n,n')^{93m}Nb	46 (23 times each det.)
	Barrel irrad. channel, "Gradient Probes" [7]	27	^{54}Fe(n,p)^{54}Mn; ^{93}Nb(n,n')^{93m}Nb	12 (2x3 times each det.)
Swiss BWR/ PSI NES Hotlab	Set 1 Surveillance capsule (to be publ.)	11	^{54}Fe(n,p)^{54}Mn; ^{93}Nb(n,n')^{93m}Nb; ^{63}Cu(n,α)^{60}Co	12 (4 times each det.)
	Set 2 Fluence monitors; RPV cavity [8]	4×1	^{54}Fe(n,p)^{54}Mn; ^{93}Nb(n,n')^{93m}Nb	7 (3 times ^{54}Fe and 4 times ^{93}Nb)
	Set 3 Fluence monitors; RPV cavity [9]	2	^{54}Fe(n,p)^{54}Mn; ^{93}Nb(n,n')^{93m}Nb	2 (1 time each det.)
OECD/ NEA/WPRS SINBAD reactor shielding benchmarks (PWRs)	HBR2-surveillance capsule [10]	9	^{237}Np(n,f)^{137}Cs; ^{238}U(n,f)^{137}Cs; ^{58}Ni(n,p)^{58}Co; ^{54}Fe(n,p)^{54}Mn; ^{46}Ti(n,p)^{46}Sc; ^{63}Cu(n,a)^{60}Co	6 (1 time each det.)
	HBR2-RPV cavity [10]	9	^{237}Np(n,f)^{137}Cs; ^{238}U(n,f)^{137}Cs; ^{58}Ni(n,p)^{58}Co; ^{54}Fe(n,p)^{54}Mn; ^{46}Ti(n,p)^{46}Sc; ^{63}Cu(n,a)^{60}Co	6 (1 time each det.)
	PCA-Replica [11]	NA	^{115}In(n,n')^{115m}In; ^{32}S(n,p)^{32}P	6 (3 times each det.)
Total number of C/E values				**109**

Illustration on the PWR RPV related validation results

N	NDL-transport	Validation case	C/E	ND-transport, %	ND-detector, %	ND-total, %
1	E-7.1	PWR_BAR_Fe54	0.993	6.6	2.2	7.0
2	E-7.1	PWR_BAR_Nb93	1.050	7.0	4.4	8.3
3	E-7.1	PWR_RPV_Fe54	1.030	11.0	2.2	11.2
4	E-7.1	PWR_RPV_Nb93	1.034	10.8	4.4	11.7
5	E-7.0	HBR2_Np237	0.938	8.0	1.7	8.2
6	E-7.0	HBR2_U238	0.870	8.0	2.0	8.2
7	E-7.0	HBR2_Ni58	0.885	8.0	1.7	8.2
8	E-7.0	HBR2_Fe54	0.899	8.0	2.1	8.3
9	E-7.0	HBR2_Ti46	0.981	9.0	3.1	9.5
10	E-7.0	HBR2_Cu63	0.862	11.0	2.8	11.4
11	E-7.1	PCA_In115	0.963	7.0	7.2	10.0
12	E-7.1	PCA_S32	0.935	6.0	6.4	8.7

For the ND uncertainties propagation in the neutron transport calculations the covariance matrices (CM) of ENDF/B-VII.1 (“E-7.1) were used for all cases with NUSS

The detector related ND uncertainties were propagated deterministically

Average C/E-1 = -4.7%

Pearson correlation coefficients for the selected quantities of interest

		PWR_Bar_dpa	PWR_RPV_dpa	**PWR_Bar_FNF**	**PWR_RPV_FNF**	PWR_BAR_Fe54	PWR_BAR_Nb93	PWR_RPV_Fe54	PWR_RPV_Nb93	HBR2_Np237	HBR2_U238	HBR2_Ni58	HBR2_Fe54	HBR2_Ti46	HBR2_Cu63	PCA_In115	PCA_S32	PETALE_Rh103	PETALE_In115	PETALE_Ni58	PETALE_Fe54
		1	2	3	4	5	6	7	8	9	10	11	12	13	14	15	16	17	18	19	20
PWR_Bar_dpa	1	1.00	0.88	0.96	0.86	0.95	0.99	0.76	0.88	0.91	0.87	0.81	0.78	0.57	0.41	0.62	0.60	0.81	0.86	0.86	0.85
PWR_RPV_dpa	2	0.88	1.00	0.84	0.95	0.92	0.88	0.94	0.99	0.88	0.88	0.88	0.86	0.70	0.57	0.79	0.85	0.57	0.59	0.61	0.61
PWR_Bar_FNF	3	0.96	0.84	1.00	0.90	0.87	0.98	0.68	0.87	0.94	0.89	0.74	0.71	0.51	0.37	0.70	0.54	0.73	0.86	0.81	0.79
PWR_RPV_FNF	4	0.86	0.95	0.90	1.00	0.84	0.89	0.85	0.98	0.93	0.91	0.81	0.78	0.63	0.52	0.87	0.78	0.50	0.62	0.58	0.57
PWR_BAR_Fe54	5	0.95	0.92	0.87	0.84	1.00	0.94	0.87	0.90	0.84	0.83	0.87	0.85	0.68	0.52	0.57	0.67	0.76	0.74	0.82	0.83
PWR_BAR_Nb93	6	0.99	0.88	0.98	0.89	0.94	1.00	0.74	0.89	0.93	0.89	0.80	0.77	0.56	0.40	0.66	0.59	0.78	0.86	0.85	0.84
PWR_RPV_Fe54	7	0.76	0.94	0.68	0.85	0.87	0.74	1.00	0.92	0.73	0.76	0.86	0.86	0.80	0.70	0.65	0.83	0.49	0.45	0.53	0.53
PWR_RPV_Nb93	8	0.88	0.99	0.87	0.98	0.90	0.89	0.92	1.00	0.91	0.90	0.86	0.84	0.68	0.56	0.83	0.84	0.54	0.60	0.61	0.60
HBR2_Np237	9	0.91	0.88	0.94	0.93	0.84	0.93	0.73	0.91	1.00	0.98	0.84	0.80	0.60	0.47	0.80	0.67	0.59	0.72	0.70	0.68
HBR2_U238	10	0.87	0.88	0.89	0.91	0.83	0.89	0.76	0.90	0.98	1.00	0.90	0.87	0.68	0.54	0.78	0.71	0.55	0.66	0.67	0.66
HBR2_Ni58	11	0.81	0.88	0.74	0.81	0.87	0.80	0.86	0.86	0.84	0.90	1.00	1.00	0.88	0.74	0.62	0.74	0.57	0.57	0.66	0.66
HBR2_Fe54	12	0.78	0.86	0.71	0.78	0.85	0.77	0.86	0.84	0.80	0.87	1.00	1.00	0.91	0.77	0.58	0.73	0.56	0.55	0.64	0.65
HBR2_Ti46	13	0.57	0.70	0.51	0.63	0.68	0.56	0.80	0.68	0.60	0.68	0.88	0.91	1.00	0.96	0.42	0.60	0.40	0.39	0.47	0.48
HBR2_Cu63	14	0.41	0.57	0.37	0.52	0.52	0.40	0.70	0.56	0.47	0.54	0.74	0.77	0.96	1.00	0.33	0.49	0.26	0.26	0.34	0.34
PCA_In115	15	0.62	0.79	0.70	0.87	0.57	0.66	0.65	0.83	0.80	0.78	0.62	0.58	0.42	0.33	1.00	0.85	0.21	0.35	0.26	0.24
PCA_S32	16	0.60	0.85	0.54	0.78	0.67	0.59	0.83	0.84	0.67	0.71	0.74	0.73	0.60	0.49	0.85	1.00	0.28	0.24	0.27	0.27
PETALE_Rh103	17	0.81	0.57	0.73	0.50	0.76	0.78	0.49	0.54	0.59	0.55	0.57	0.56	0.40	0.26	0.21	0.28	1.00	0.92	0.87	0.86
PETALE_In115	18	0.86	0.59	0.86	0.62	0.74	0.86	0.45	0.60	0.72	0.66	0.57	0.55	0.39	0.26	0.35	0.24	0.92	1.00	0.89	0.87
PETALE_Ni58	19	0.86	0.61	0.81	0.58	0.82	0.85	0.53	0.61	0.70	0.67	0.66	0.64	0.47	0.34	0.26	0.27	0.87	0.89	1.00	1.00
PETALE_Fe54	20	0.85	0.61	0.79	0.57	0.83	0.84	0.53	0.60	0.68	0.66	0.66	0.65	0.48	0.34	0.24	0.27	0.86	0.87	1.00	1.00

If only highly "representative" data selected for validation (r>0.8), the average C/E-1 = -3.0%

Illustration on the PWR RPV FNF assessment

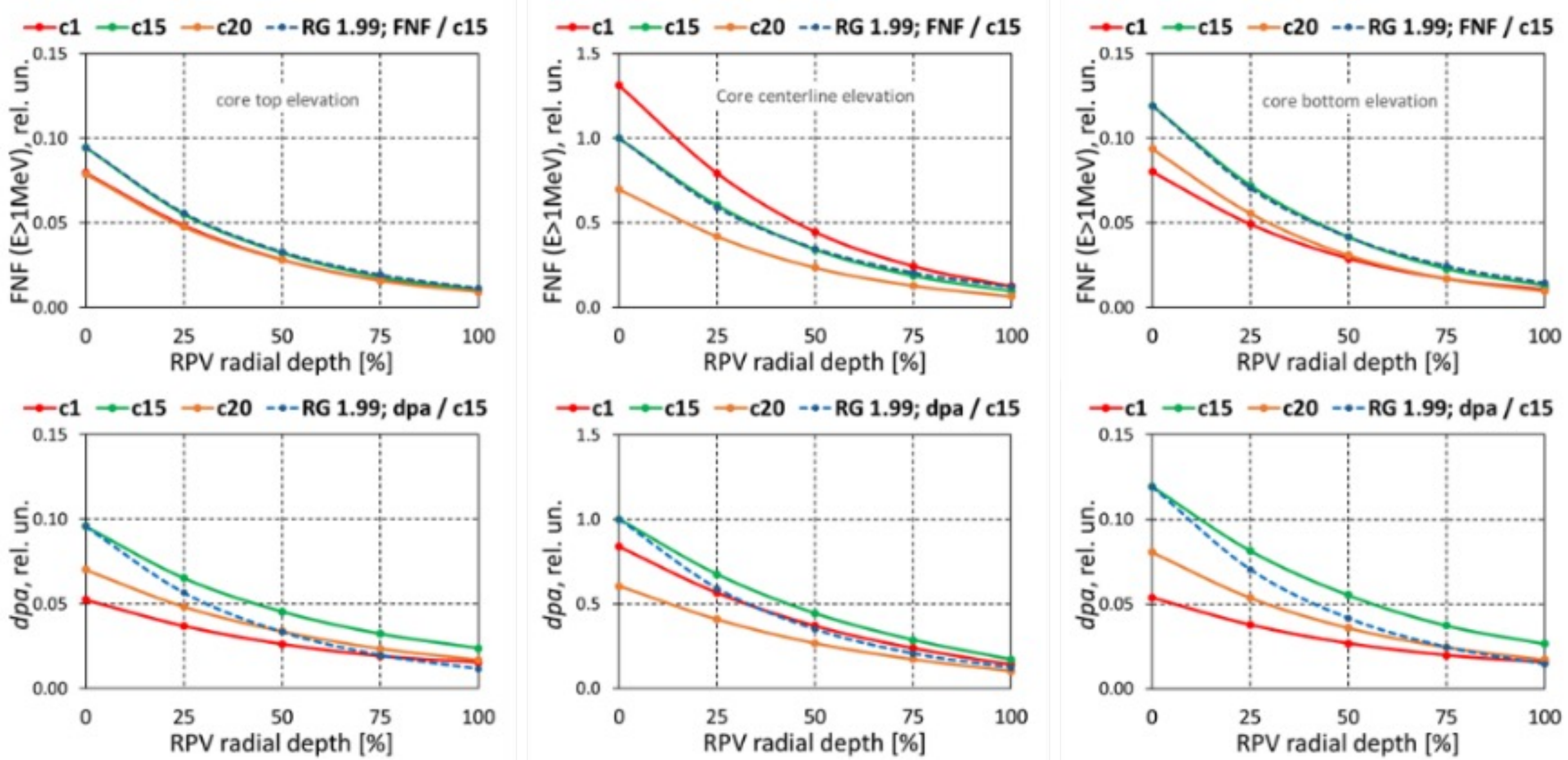

FNF and *dpa* attenuation inside the PWR RPV wall for selected reactor cycles; normalized.

Best estimate plus uncertainty (BEPU) FNF and *dpa* assessments at zones outside the beltline height are more appropriate than simplified evaluations based on generic approximations

Towards the calculation scheme and models further upgrading

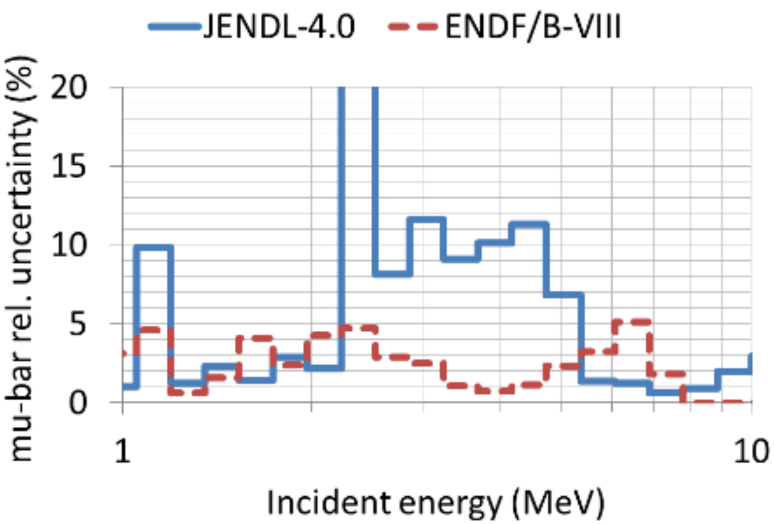

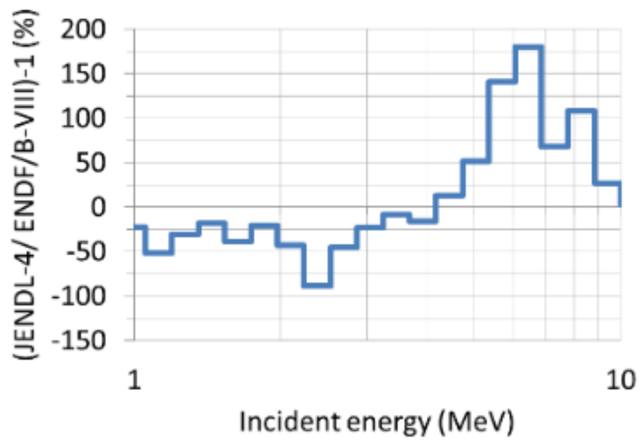

Information from the modern NDLs; left - mu-bar uncertainties; right – ration of the mu-bars

Model	PWR-GP	PWR-ST	BWR-D
σ^{FNF}, (%) / "Sandwich rule"	5 (E>0.1MeV)	NA	12
σ^{FNF}, (%) / NUSS (+nubar, +chi)	8*	11*	15*
MAX(|C/E-1|), (%)	15	15	20 (15)
<C/E-1>, Fe-54, (%)	5*	5*	18* (-1)
<C/E-1>, Nb-93, (%)	-1*	3*	9* (-9)

For RPV FNF assessments, just the differences between the JENDL-4.0 and ENDF/B-VII.1 libraries for the angular distributions of $^{16}O(n,n)$ lead to the differences of ~10% for PWR and ~20% for BWR

Need for detailed irradiation history

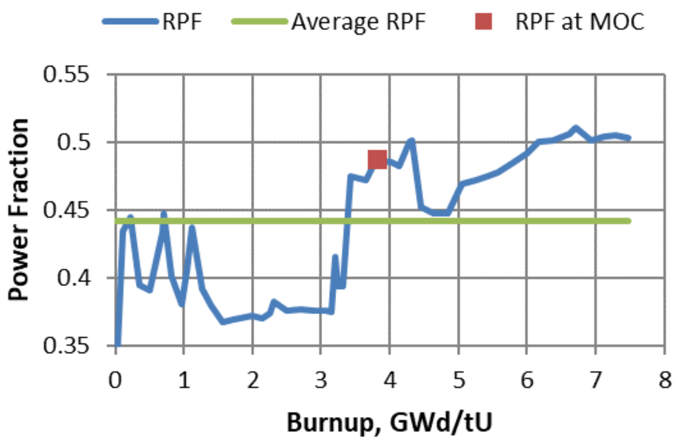

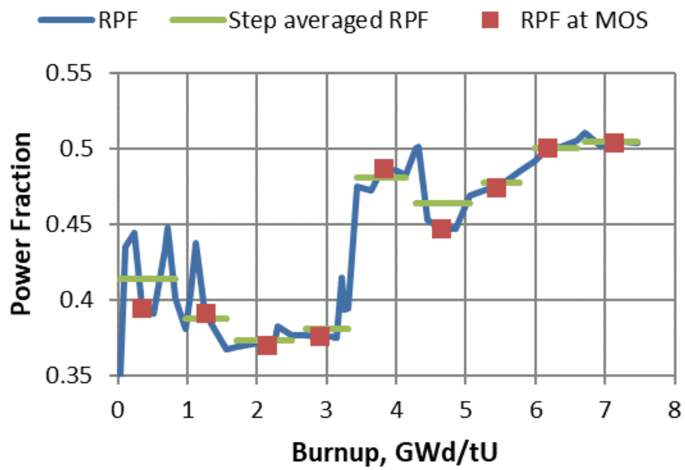

Detailed RPF behavior of a specific node in comparison with Middle-of-Cycle (MOC) RPF, cycle-average RPF and several Middle-of-Step (MOS) RPF values

Subdivision of the entire cycle irradiation history into shorter time/BU steps allows noticeably more accurate dosimetry assessments

PAUL SCHERRER INSTITUT

Summary

- Several experimental campaigns were performed in Switzerland for validation of RPV FNF assessments, in collaboration of the Swiss utilities, PSI and the reactor vendor companies, for both PWR and BWR reactors
- A “similarity analysis” has been performed using NUSS NDUQ capability, demonstrating applicability of the available experimental data for RPV FNF validation, as well showing similarity of the PSI proprietary models with selected publicly open SINBAD reactor shielding benchmarks - HBR-II, PCA-Replica
- In general, very reasonable C/E results have been achieved ($0.8<C/E<1.2$), taking into account the associated experimental and calculation uncertainties

Summary

Further methodology upgrades should be relevant for LWRs LTO and the following tasks are proposed for realization:

- Upgrade the CASMO/SIMULATE/MCNP+FISPACT scheme to CASMO/SIMULATE/**SNF**/MCNP+FISPACT for explicit 3D neutron source strength and spectrum specifications
- Implement an automatized procedure for optimized step-wise representation of the operating history and the neutron source in the MCNP models, based on the core-follow CASMO5/SIMULATE5 information
- When become available, the angular scattering distributions’ uncertainties will be necessary to include into the NDUQ assessments

So far, the coolant density/temperature in the KKG PWR core bypass region was preliminary investigated at PSI with OpenFOAM CFD models and this capability should be further advanced for BEPU RPV FNF simulations

PAUL SCHERRER INSTITUT PSI

Wir schaffen Wissen – heute für morgen

My thanks go to

- Swissnuclear
- PSI/NES Hotlab
- KKL
- KKG
- LRS/EPFL